

Stepwise Collapse of a Giant Pore Metal–Organic Framework

SUPPLEMENTARY INFORMATION

Adam F. Sapnik,^a Duncan N. Johnstone,^a Sean M. Collins,^{a,b} Giorgio Divitini,^a Alice M. Bumstead,^a Christopher W. Ashling,^a Philip A. Chater,^c Dean S. Keeble,^c Timothy Johnson,^d David A. Keen,^e Thomas D. Bennett^{*a}

^a Department of Materials Science and Metallurgy, University of Cambridge, Cambridge, CB3 0FS, UK.

^b School of Chemical and Process Engineering & School of Chemistry, University of Leeds, Leeds, LS2 9JT, UK.

^c Diamond Light Source Ltd, Diamond House, Harwell Campus, Didcot, Oxfordshire, OX11 0DE, UK.

^d Johnson Matthey Technology Centre, Blount's Court, Sonning Common, RG4 9NH, UK.

^e ISIS Facility, Rutherford Appleton Laboratory, Harwell Campus, Didcot, Oxfordshire, OX11 0QX, UK.

* To whom correspondence should be addressed; E-mail: tdb35@cam.ac.uk

SUPPLEMENTARY INFORMATION

Pawley Refinement of MIL-100 (Fe).....	3
Powder X-ray Diffraction Data	4
Scanning Electron Microscopy	5
High-Resolution Scanning Transmission Electron Microscopy.....	6
Hematite Powder X-ray Diffraction Data	8
Fourier-Transform Infrared Spectroscopy.....	9
CHN Analysis	9
X-ray Total Scattering Structure Factors	10
X-ray Pair Distribution Functions	11
BET Surface Areas and Total Pore Volumes	11
Logarithmic Nitrogen Adsorption Isotherms.....	12
NL-DFT Pore Size Analysis	12
Thermogravimetric Analysis – Solvent Stabilisation	13
Scanning Electron Microscopy – Solvent Stabilisation	14
X-ray Pair Distribution Functions – Solvent Stabilisation	15
Logarithmic Nitrogen Adsorption Isotherms – Solvent Stabilised.....	15
BET Surface Areas and Total Pore Volumes – Solvent Stabilisation.....	16
NL-DFT Pore Size Analysis – Solvent Stabilisation	16
References	16

Pawley Refinement of MIL-100 (Fe)

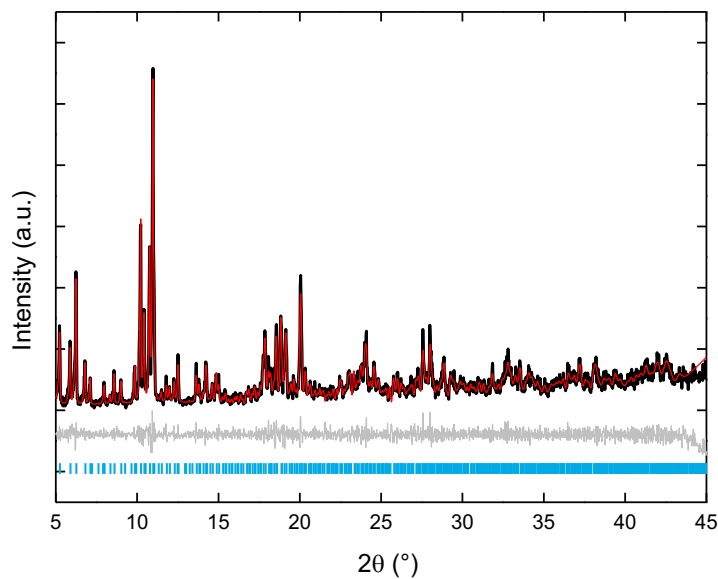


Figure S1 Pawley refinement of MIL-100 (Fe). Experimental data (black), calculated diffraction pattern (red), difference function (grey) and symmetry-allowed reflections (blue). Symmetry allowed reflections were calculated from the reported crystallographic information file in Ref. 1.

Table S1 Crystallographic data from Pawley refinement of MIL-100.

$R_{wp} = 9.48$	Experimental	Reported [1]
$a = b = c$	73.25(3)	73.340(1)
$\alpha = \beta = \gamma$	90	90

Powder X-ray Diffraction Data

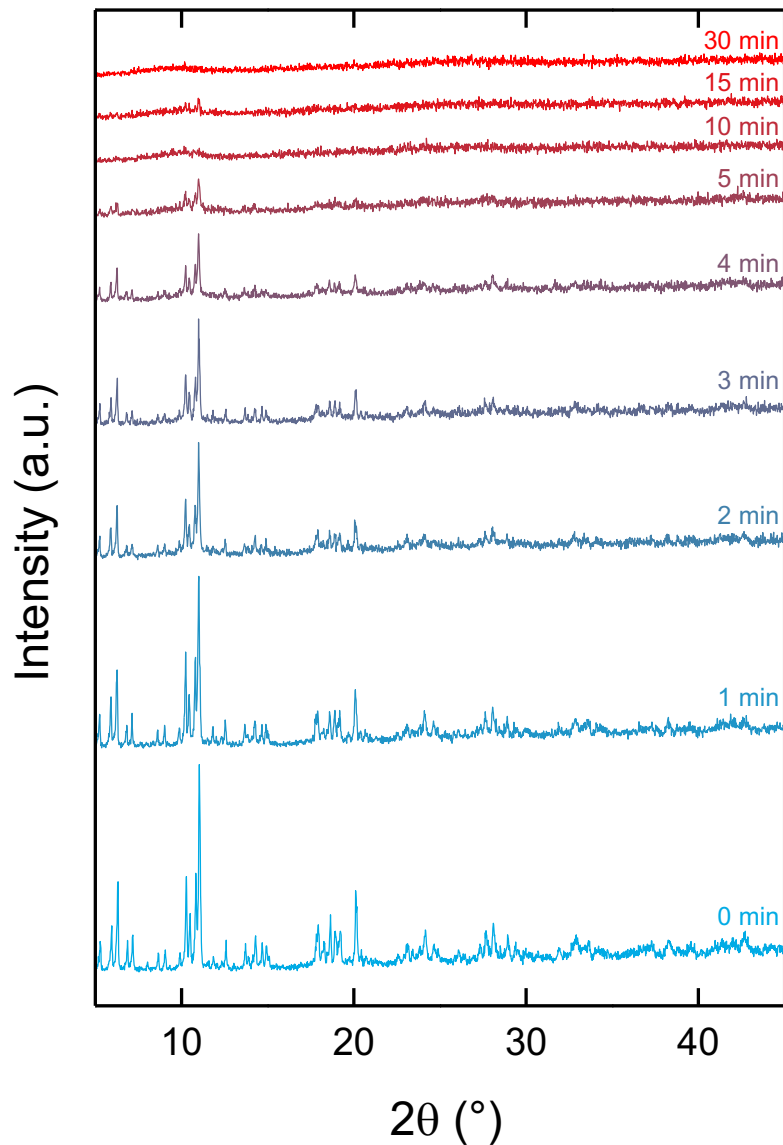


Figure S2 Powder X-ray diffraction patterns of MIL-100 as a function of duration of ball milling.

Table S2 Integrated area of the, background subtracted, (333) Bragg peak relative to MIL-100.

Time (min)	Integrated area (%)
0	100
1	91.2
2	56.7
3	47.9
4	34.9
5	18.5
10	4.80
15	5.70
30	0

Scanning Electron Microscopy

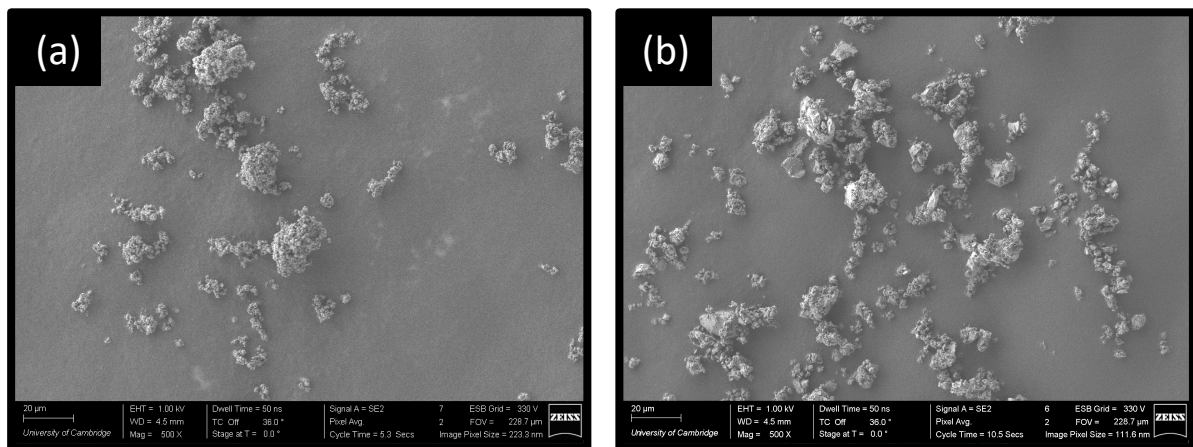


Figure S3 Scanning electron microscopy images of (a) MIL-100 and (b) α_mMIL-100.

High-Resolution Scanning Transmission Electron Microscopy

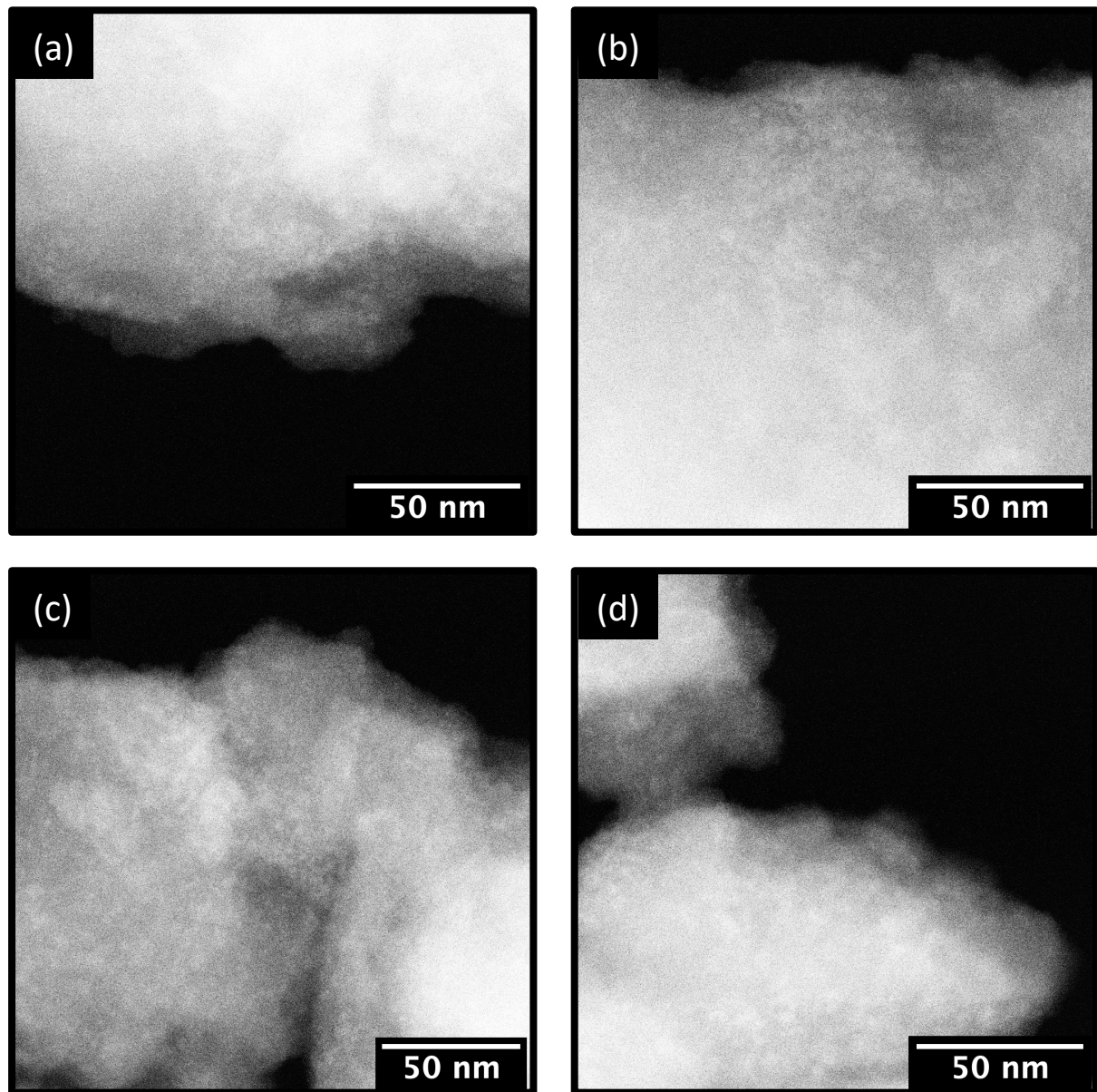


Figure S4 High-angle annular dark-field HR-STEM images of a_m MIL-100 (Fe) (a-d), none of which exhibited lattice fringes.

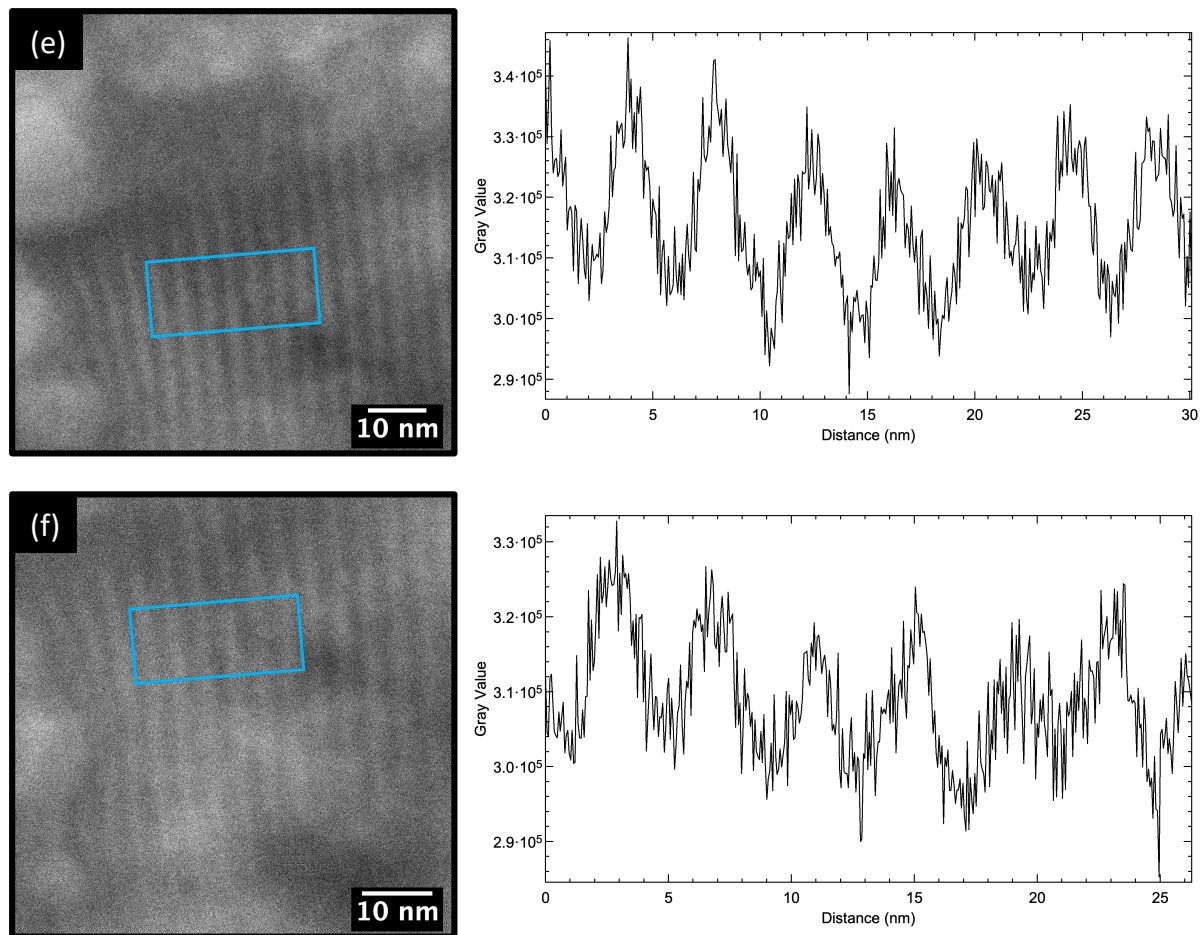


Figure S4 Bright field (e) and high-angle annular dark-field (f) HR-STEM images of MIL-100 and their corresponding line profile measurements of the highlighted lattice fringes.

Hematite Powder X-ray Diffraction Data

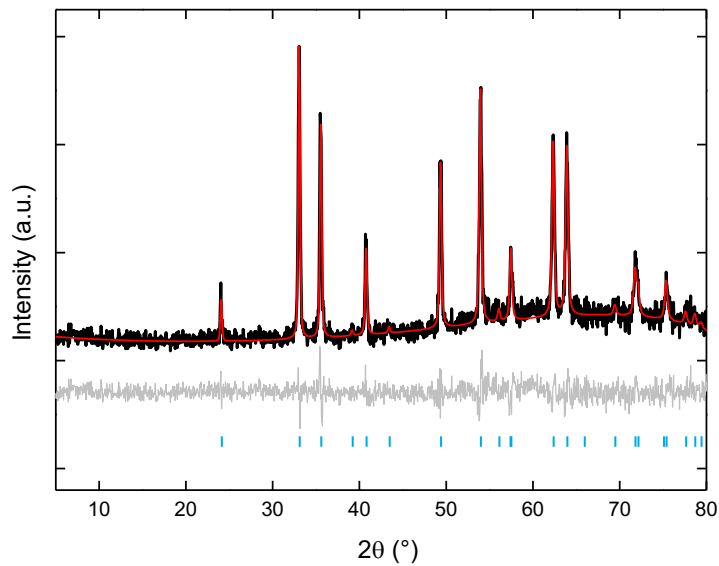


Figure S5 Pawley refinement of powder X-ray diffraction data from the bright orange residue from TGA analysis. Experimental data (black) calculated diffraction pattern (red), difference curve (grey) and symmetry-allowed reflections for hematite (blue). Symmetry allowed reflections were calculated from the reported crystallographic information file in Ref. 2.

Table S3 Crystallographic data from Pawley refinement of hematite.

$R_{wp} = 17.63$	Experimental	Reported [2]
$a = b$	5.04(3)	5.038(2)
c	13.77(4)	13.772(12)
$\alpha = \beta$	90	90
γ	120	120

Fourier-Transform Infrared Spectroscopy

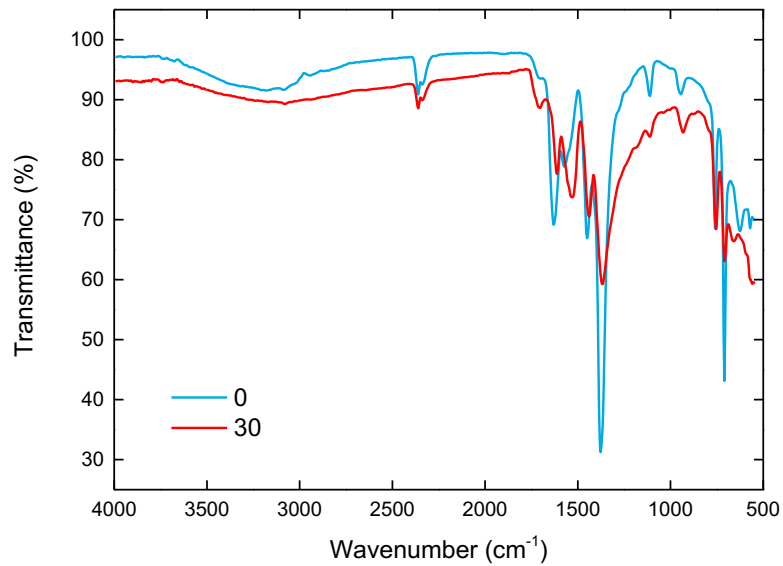


Figure S6 FT-IR spectra of MIL-100 (blue) and a_m MIL-100 (red). Key shows duration of ball milling in minutes.

CHN Analysis

Table S4 CHN analysis of the MIL-100 materials.

Time (min)	C %	H %	N %
0	28.8	1.93	0.55
1	26.9	2.12	0.53
2	28.1	2.19	0.51
3	27.9	2.12	0.5
4	28.7	2.06	0.91
5	28.7	2.04	0.91
10	29.7	1.92	0.96
15	28.4	2.15	0.65
30	29.5	2.04	0.91

X-ray Total Scattering Structure Factors

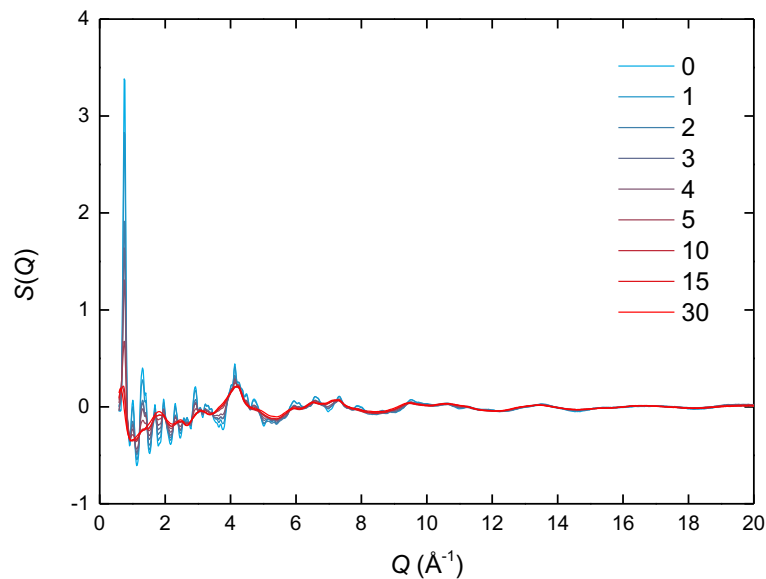


Figure S7 X-ray total scattering structure factors for the MIL-100 materials. Key shows duration of ball milling in minutes.

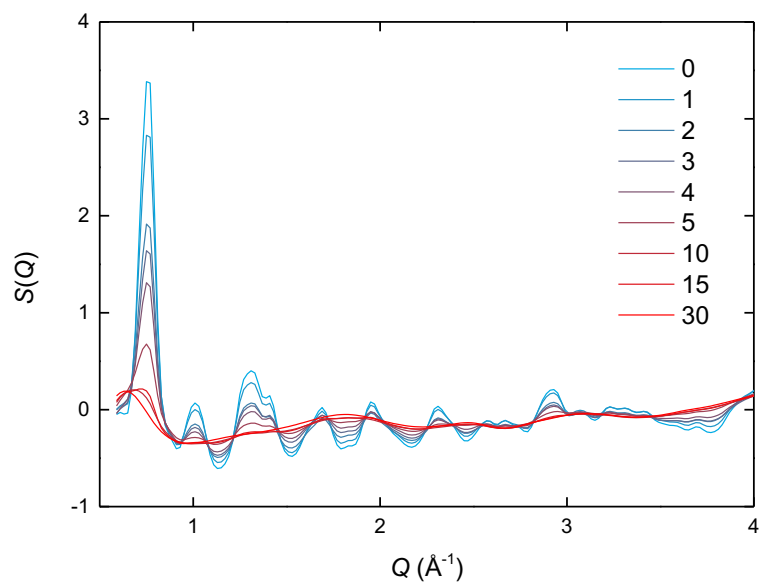


Figure S8 Low- Q region of the X-ray total scattering structure factors for the MIL-100 materials. Key shows duration of ball milling in minutes.

X-ray Pair Distribution Functions

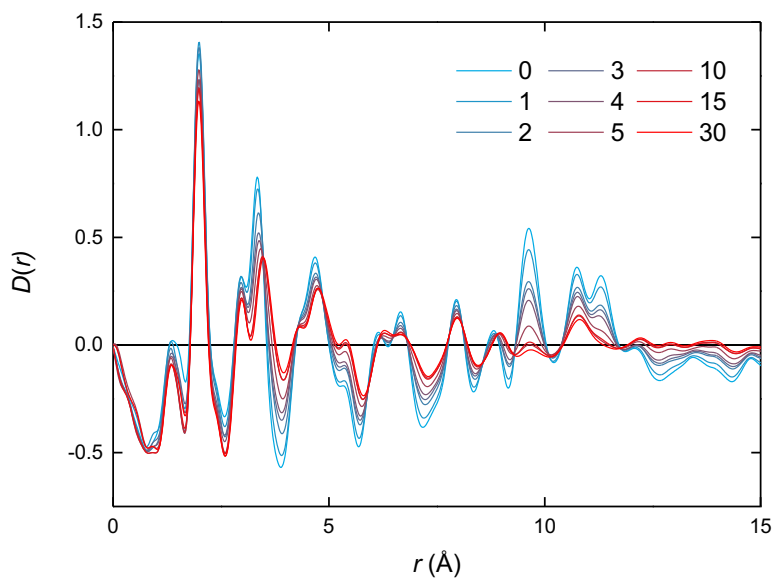


Figure S9 Low-r region of the pair distribution functions for the MIL-100 materials. Key shows duration of ball milling in minutes.

BET Surface Areas and Total Pore Volumes

Table S5 BET surface area, maximal nitrogen uptake and total pore volume as derived from nitrogen adsorption isotherms for the MIL-100 materials. Maximal uptake taken from $p/p_0 \approx 0.98$. The BET surface area of the 10 min sample could not be calculated whilst following the Rouquerol consistency criteria.

Time (min)	BET Surface Area ($\text{m}^2 \text{ g}^{-1}$)	Maximal uptake ($\text{cm}^3 \text{ g}^{-1}$)	Total pore volume ($\text{cm}^3 \text{ g}^{-1}$)
0	2240(18)	641.0	0.991
1	673(2)	231.2	0.357
2	417(2)	150.0	0.231
3	401(3)	149.0	0.230
5	101.7(7)	57.2	0.088
10	-	38.5	0.060
15	36.7(2)	42.8	0.066
30	2.02(3)	31.7	0.049

Logarithmic Nitrogen Adsorption Isotherms

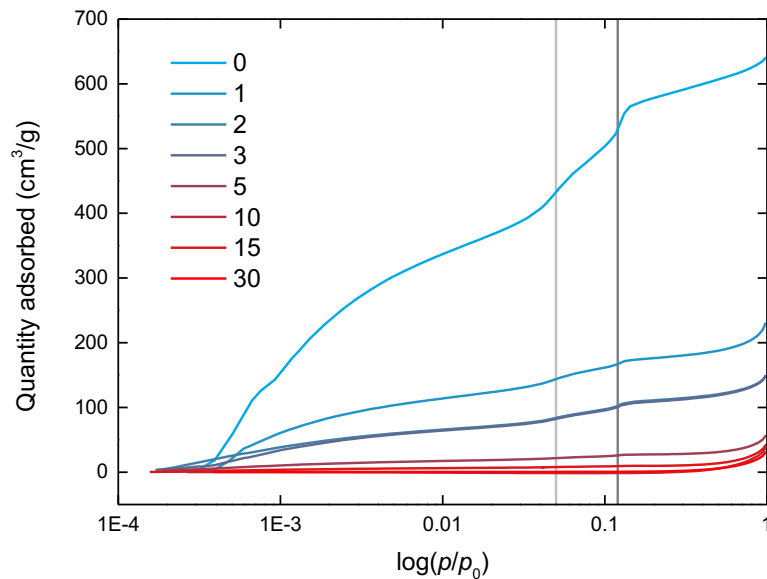


Figure S10 Nitrogen adsorption isotherms of the MIL-100 materials, expressed on a logarithmic scale to emphasise the filling of the small and large pores at approximately 0.05 (light grey guideline) and 0.12 p/p_0 (dark grey guideline). For clarity the desorption branch has been omitted. Key shows duration of ball milling in minutes.

NL-DFT Pore Size Analysis

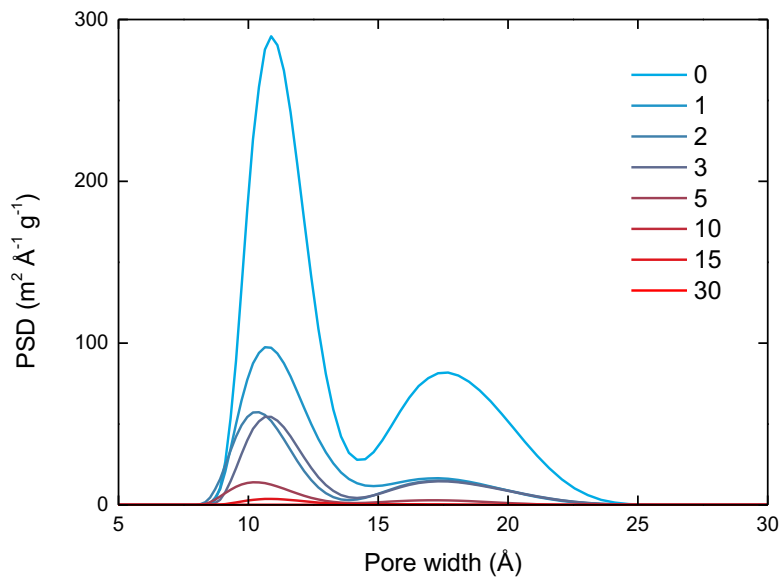


Figure S11 Pore size distributions determined from nitrogen adsorption isotherms using NL-DFT. Key shows duration of ball milling in minutes.

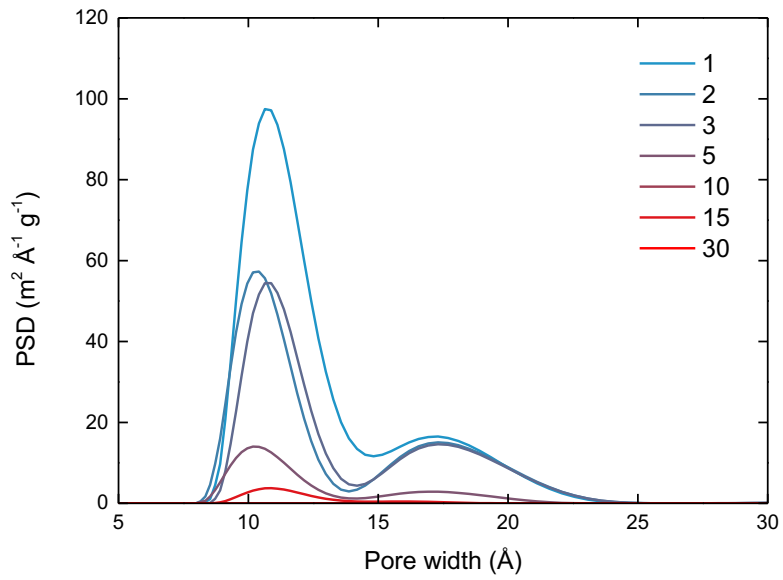


Figure S12 Pore size distributions determined from nitrogen adsorption isotherms using NL-DFT, MIL-100 is excluded here in order to emphasise the ball-milled materials. Key shows duration of ball milling in minutes.

Thermogravimetric Analysis – Solvent Stabilisation

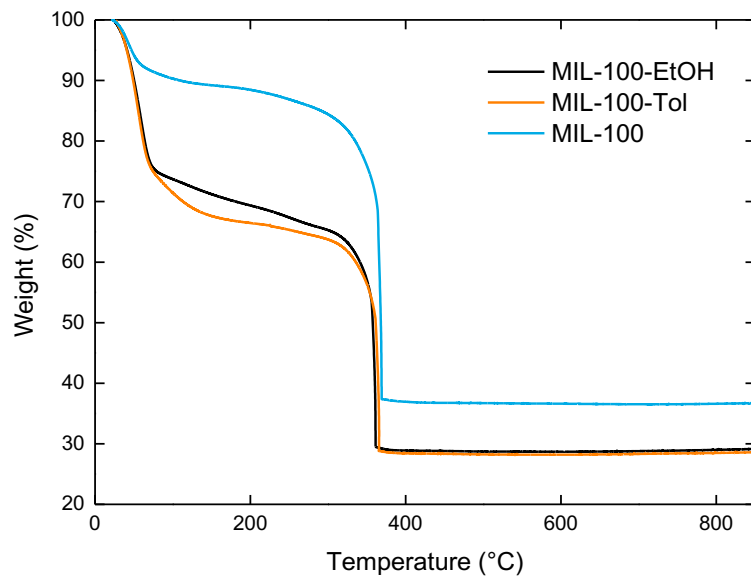


Figure S13 Thermogravimetric analysis of non-stabilised MIL-100 (blue), ethanol stabilised (black) and toluene stabilised (orange) MIL-100.

Scanning Electron Microscopy – Solvent Stabilisation

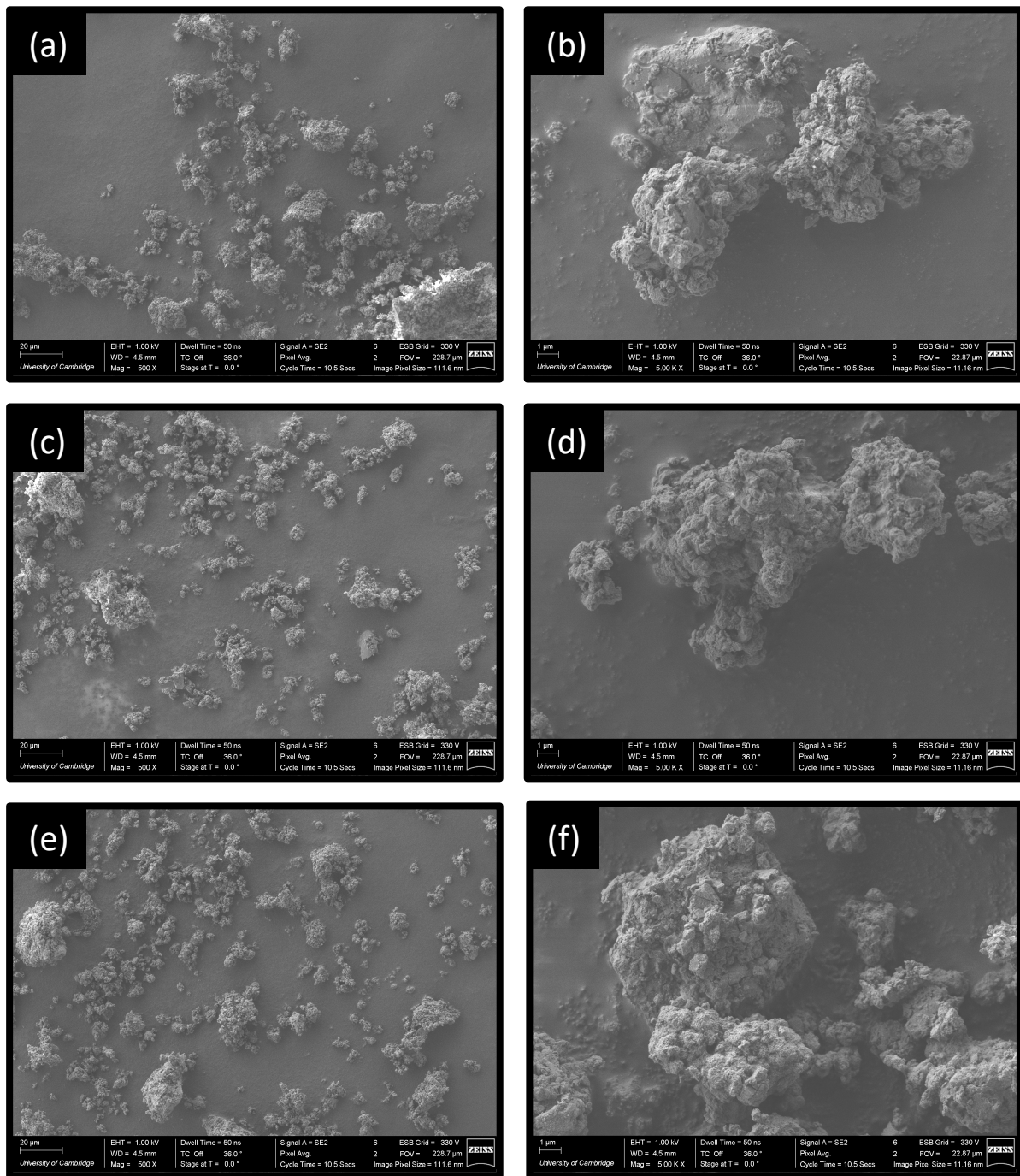


Figure S14 Scanning electron microscopy images of non-stabilised MIL-100 (a-b), MIL-100-EtOH (c-d) and MIL-100-Tol (e-f) all after one minute of ball milling.

X-ray Pair Distribution Functions – Solvent Stabilisation

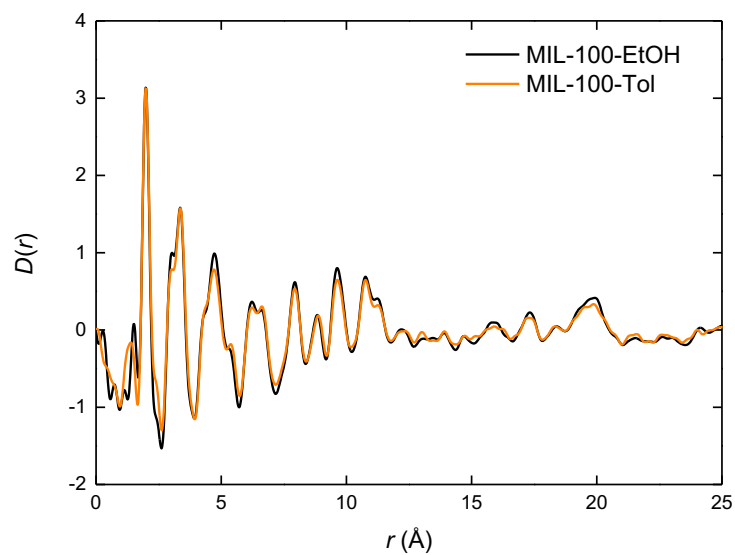


Figure S15 X-ray pair distribution functions for the solvent-stabilised materials.

Logarithmic Nitrogen Adsorption Isotherms – Solvent Stabilised

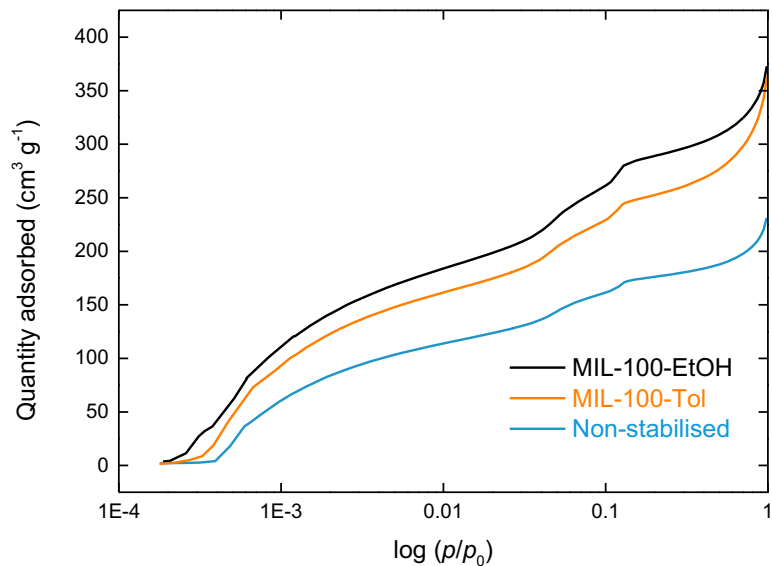


Figure S16 Nitrogen adsorption isotherms of the solvent-stabilised MIL-100 materials expressed on a logarithmic scale. For clarity the desorption branch has been omitted.

BET Surface Areas and Total Pore Volumes – Solvent Stabilisation

Table S6 BET surface area, maximal nitrogen uptake and total pore volume as derived from nitrogen adsorption isotherms for solvent stabilised MIL-100. Maximal uptake taken from $p/p_0 \approx 0.98$.

Solvent	BET Surface Area ($\text{m}^2 \text{g}^{-1}$)	Maximal uptake ($\text{cm}^3 \text{g}^{-1}$)	Total pore volume ($\text{cm}^3 \text{g}^{-1}$)
Ethanol	1101(5)	372.8	0.575
Toluene	966(4)	362.8	0.560

NL-DFT Pore Size Analysis – Solvent Stabilisation

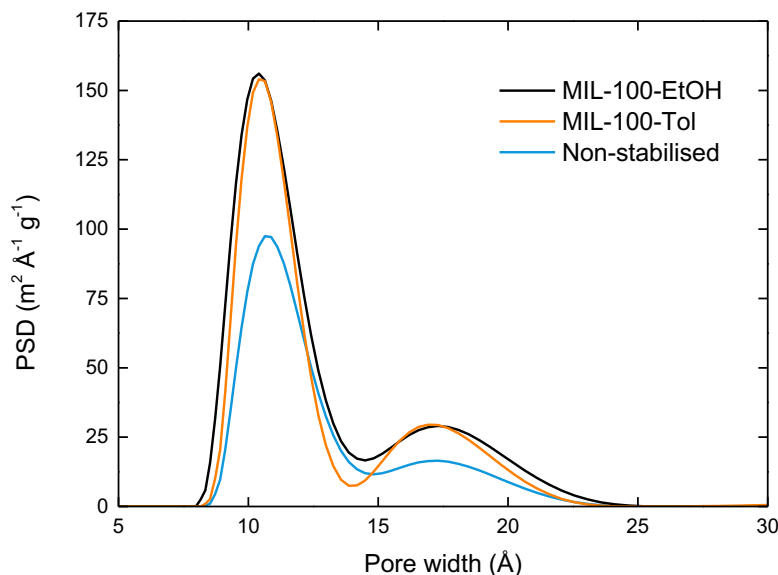


Figure S17 Pore size distributions of MIL-100 1 min (blue), MIL-100-EtOH (black) and MIL-100-Tol (orange) determined from nitrogen adsorption isotherms using NL-DFT.

References

- 1 P. Horcajada, S. Surblé, C. Serre, D. Y. Hong, Y. K. Seo, J. S. Chang, J. M. Grenèche, I. Margiolaki and G. Férey, *Chem. Commun.*, 2007, **100**, 2820–2822.
- 2 R. L. Blake, R. E. Hessevick, T. Zoltai and L. W. Finger, *Am. Mineral.*, 1966, **51**, 123–129.